

## Theoretical research into operation of rotary potato harvester

J. Olt<sup>1,\*</sup>, V. Bulgakov<sup>2</sup>, V. Bonchik<sup>3</sup>, Z. Ruzhylo<sup>2</sup>, V. Volskiy<sup>4</sup>, V. Melnik<sup>5</sup>,  
Ye. Ihnatiev<sup>6</sup> and H. Kaletnik<sup>7</sup>

<sup>1</sup>Estonian University of Life Sciences, Institute of Technology, 56 Kreutzwaldi Str., EE 51006 Tartu, Estonia

<sup>2</sup>National University of Life and Environmental Sciences of Ukraine, 15 Heroyiv Oborony Str., UA 03041 Kyiv, Ukraine

<sup>3</sup>State Agrarian and Engineering University in Podilia, 13 Shevchenko Str., UA 32300 Kamenets-Podilsky, Ukraine

<sup>4</sup>National Scientific Centre, “Institute for Agricultural Engineering and Electrification”, 11 Vokzalna Str., Glevakcha 1, Vasylkiv District, UA 08631 Kyiv Region, Ukraine

<sup>5</sup>Kharkiv Petro Vasilenko National Technical University of Agriculture, 44 Alchevskih Str., UA 61002 Kharkiv, Ukraine

<sup>6</sup>Dmytro Motornyi Tavria State Agrotechnological University, 18<sup>B</sup> Khmelnytsky Ave, UA 72310, Melitopol, Zaporozhye Region, Ukraine

<sup>7</sup>Vinnytsia National Agrarian University of Ukraine, 3 Soniacha Str., UA21008 Vinnytsia, Ukraine

\*Correspondence: [jyri.olt@emu.ee](mailto: jyri.olt@emu.ee)

Received: May 25<sup>th</sup>, 2021; Accepted: June 22<sup>nd</sup>, 2021; Published: June 28<sup>th</sup>, 2021

**Abstract.** The topic of the paper is the determination and justification of the rational design and kinematic parameters of clod breaking tools in rotary potato harvesters with the aim of improving their separating efficiency. A new mathematical model has been developed for the motion of a soil particle on the working surfaces of the cone-shaped and cylindrical vanes in the rotary tool of the new design developed by the authors. Differential equations have been generated for the motion of a soil clod as a material particle from the moment of its arrival to the surface of the vane until the moment of its departure from the said surface. As a result of the completed investigations, relations have been established between the time of contact and absolute displacement of the soil particle and the velocity of its departure from the rotor vane surface, on the one hand, and the kinematic and design parameters of the rotor, on the other hand. For example, when the machine translation velocity increases, the absolute displacement of the soil particle within the interval from the time zero to the moment of its departure from the vane surface increases from 0.59 m to 0.65 m, the velocity of soil particle departure from the vane surface - from 1.61 m s<sup>-1</sup> to 1.81 m s<sup>-1</sup>. The highest values of the absolute displacement of the soil particle and the velocity of its departure from the vane surface are achieved at a machine translation velocity of 2.0 m s<sup>-1</sup>. The time of the contact between the material particle and the vane surface decreases with the rise of the translation velocity. When the rotor rotation frequency varies within the range from 20 min<sup>-1</sup> to 100 min<sup>-1</sup>, the absolute velocity, with which the soil particle leaves the vane surface, rises to 4 m s<sup>-1</sup>. The duration of the contact between the material particle and

the vane reaches its maximum value of 0.33 s, when the rotor rotation frequency varies within the range of 30–40 min<sup>-1</sup>.

**Key words:** clod-crushing, harvesting machine, loamy soil, potato, soil separation, vertical rotor.

## INTRODUCTION

The separation of tubers from soil clods is a very important operation in the process of harvesting potatoes, especially in case of potato harvesters working on heavy loam soils (Peters, 1997; Bishop et al., 2012; Wei et al., 2017). In such soils, the soil clods are hard to break, which results in their arrival together with tubers onto the potato harvester separating tools, where their separation is rather complicated. That applies, first of all, to the soil clods of the size that is equal to or greater than the size of the tubers. In that case, the soil content in the potato heap arriving to the hopper exceeds 20%, which does not meet the agronomical standards. When operating on heavy loam soils, the potato heap cleanness rate does not exceed 55–74%, while the tuber damage rate varies within the range of 18–25% (Lü et al., 2015; Bulgakov et al., 2020; Ruzhylo et al., 2020).

In view of the above-said, the need arises to disintegrate the soil clods already at the stage of tuber lifting, i.e. prior to their arrival onto the cleaning tools. Meeting these conditions will facilitate raising the efficiency of use of combined units on heavy soils and reducing the potato tuber loss and damage rates (Bulgakov et al., 2019).

The fundamental basis for the research into the laws governing the process of soil clod disintegration in relation to the mechanical factors is outlined in the studies by the prominent scientists: Vasilenko (1996; 1998), Petrov (2004), Ruyschaert et al. (2006); Gao et al., 2011; Ichiki et al., 2013; Lü et al. (2015, 2017), Feng et al. (2017); Wang et al. (2017); Xin & Liang (2017); Bulgakov et al. (2018a, 2018b, 2018c, 2019), Nowak et al. (2019); Siberev et al. (2019); Wei et al. (2019a, 2019b), Issa et al. (2020); Ruzhylo et al., 2020.

The studies have established that the efficiency of using the various methods of breaking soil clods depends on the mechanical strength of the said clods and the tuber damage rate. The strength of the clods, in its turn, depends on the physical and mechanical properties of the soil (Vasilenko, 1998; Petrov, 2004; Ruyschaert et al., 2006).

When analysing the interaction between the clod crushing tools and the tuber-bearing soil bed of the potato row, special attention has to be paid to the disintegration of clods under dynamic load conditions (Wei et al., 2017). In view of the above-said, similar research has been carried out with regard to the case of the collision between the tubers and clods, on the one hand, and the riddle chain surface, on the other hand. In this case, it has been suggested that dynamic clod breaking can be used at the initial stage of the work process, that is, in the zone of lifting the tuber-bearing soil slice and transferring it to the riddle chain, where the large amount of soil reliably protects the tubers from mechanical damage (Bulgakov et al., 1999).

The fundamental research into the motion of a material point on the surfaces of tools in agricultural machines is presented in the papers (Vasilenko, 1996 and 1998).

The authors have developed a new design of the rotary tool (Bulgakov et al., 2021), Ihnatiev et al., 2021; Olt et al., 2021) which provides for reducing the soil clods to sufficiently small sizes, at which they are easily separated from tubers on the potato harvester's web elevator.

The design and process schematic model of the tractor-hitched two-row potato harvester of the new design developed by the authors is presented in Fig. 1.

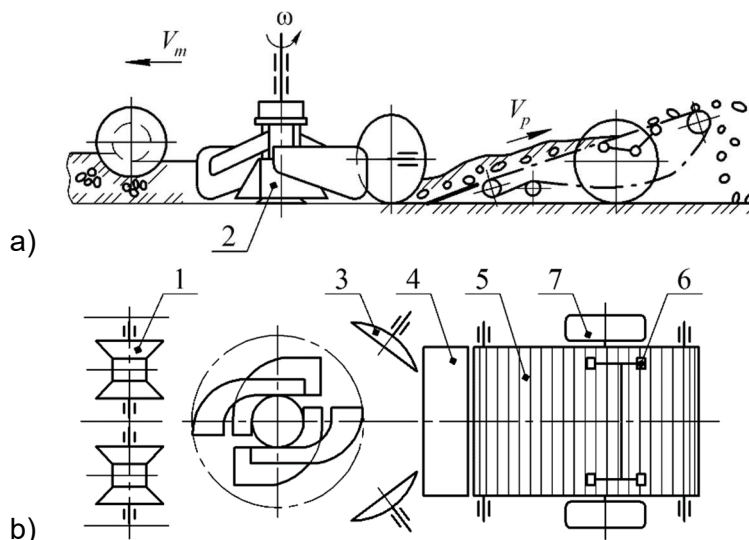


**Figure 1.** Design and process schematic model of new potato harvester: a – side view; b – top view: 1 – depth rollers; 2 – vertical rotor; 3 – spherical discs; 4 – lifting share; 5 – slat elevator; 6 – elevator belt vibrator; 7 – transport wheels (Bulgakov et al., 2021).

The work process with the use of the new potato harvester proceeds as follows. As the harvester travels in the potato field directly on the two potato rows, the depth rollers 1 press down the upper parts of the row beds, breaking them through a certain depth. The vertical rotor 2 with its upper and lower beaters rotating in the opposite directions with respect to each other and equipped with vanes travels along the centreline of the inter-row spacing between the potato rows under consideration at a pre-set depth. The travelling rotor establishes such conditions that the conically set vanes of the lower beater grasp the tuber-bearing soil beds of both the rows from below and dump them into the central part of the inter-row spacing. The tuber-bearing bed that has been completely disintegrated by the vanes of the upper beater is shifted to the centre of the inter-row spacing by the two spherical discs 3, which are set at a pre-set distance from the diameter of the rotor 2 and at an angle of attack with respect to the potato harvester motion direction. Because of the different directions of the rotary motion performed by the lower and upper beaters of the rotor, the potato heap is actively separated into different components. Also, when the tuber-bearing soil bed is shifted to the centre of the inter-row spacing by the spherical discs 3, potato tubers are extracted from the heap and cast on the surface of the inter-row spacing. After the tuber-bearing soil bed is disintegrated and partially deployed into separate components, a windrow is formed, which is picked up by the solid share 4 (the share does not dig in the soil, but only slides with its working edge on the soil surface) and fed onto the slat elevator 5. And this is the area, where the final separation of the impurities takes place, as they fall down through the openings between the slats of the elevator. In case of separating a damp potato heap, the working leg of the slat elevator 5 can be additionally put in oscillatory motion with the use of the vibrator 6, thus ensuring the high quality of cleaning potato tubers from impurities. The

frame of the machine is supported by the transport wheels 7. The machine is equipped with the devices for adjustment of the depth, at which the vertical rotor 2 runs in the soil, the rotation frequency of its lower and upper beaters as well as other adjustments. The potato tubers completely cleaned from impurities are either discharged to the area in the field, where the harvesting has been finished, or loaded to the hopper.

The tests and field experiment investigations carried out by the authors (Bulgakov et al., 2021) with the tractor-hitched potato harvester under consideration have yielded good results, which proves the achieved level of performance with regard to the quality and efficiency of potato harvesting. This achievement provides grounds for recommending the use of the described new principle of potato tuber harvesting in commercial potato harvesters.

The aim of the study was to determine and justify the rational design and kinematic parameters for the rotary tool in the potato harvester in order to improve its separating capacity, basing on the generation of a mathematical model for the motion performed by loosened soil on the vanes of the vertical rotor, the calculations with the use of the model and the analysis of the obtained results.

## MATERIALS AND METHODS

The authors have carried out theoretical investigations in order to substantiate the rational design and kinematic parameters of the discussed potato harvester.

As is known, the work process of many tools in potato harvesters, including the machine under consideration, implies the transfer of materials over their surfaces.

Therefore, in order to select the rational design parameters for the tools in the above-mentioned machines, it is necessary to determine the kinematic and dynamic parameters of the motion performed by the material on their surfaces. For that purpose, the differential equations of the motion performed by soil particles on the working surfaces of the vanes have to be generated (Kheiry et al., 2018).

When developing the mathematical model of the vertical rotor operation process, it is necessary to take into account that the motion of soil particles on the vane surfaces takes place in the continuous soil medium. For that reason, it is appropriate to assume that the soil particles move on the working surfaces of the vanes in constant contact, as distinct from the series-produced potato harvester tools, in which the tuber-bearing soil bed is disintegrated with the use of impact processes.

After the analysis of the scientific papers (Petrov, 2004; Blahovec & Židova, 2004; Hevko et al., 2016; Pshechenkov et al., 2018; Gulati & Singh, 2019) about the research into the motion of materials on the surfaces of tools in machines, it becomes obvious that the mathematical model of the vertical rotor operation process has to be generated basing on the following assumptions:

- interaction between the rotor vanes and the soil mass implies developing a complex rheological model, which takes into account the physical and mechanical properties of the material;
- in order to determine the possible displacements of the soil mass during the disintegration process (displacement of the tuber-bearing soil bed), it is necessary to regard its displacement as the displacement of a material particle;
- in view of the fact that the displaced soil interacts not only with the vane, but also with the main, undisplaced soil mass, some cases are possible, where the latter

interaction forces reduce the impact of the friction force, although, it still cannot be considered negligible.

In order to investigate the process of the soil particle moving on the working surfaces of the vanes that are offset with respect to the vertical rotation axis, it is necessary to determine theoretically the conditions for the motion of the soil particle on the cone-shaped vane and the cylindrical vane, respectively, in constant contact with them. The following assumptions have been made in the process of generating the differential equations of motion:

- velocity of the soil particle at the moment of its arrival onto the surface of the vane is equal to zero;
- angular velocity of the vane is constant;
- soil particle moves along the vane.

### Theory and modelling

The next step is to generate the differential equations of motion for the soil particle moving over the working surfaces of the vanes, first for the lower beater, then for the upper one.

The generation of equations is started with the lower beater. A vane of the lower beater performs rotary motion in the horizontal plane counter-clockwise at a constant angular velocity and also performs uniform translational motion together with the potato harvester. The first step is to design the equivalent schematic model of the motion performed by the material point  $M$  (soil particle) on the surface of the cone-shaped vane under consideration (Fig. 2).

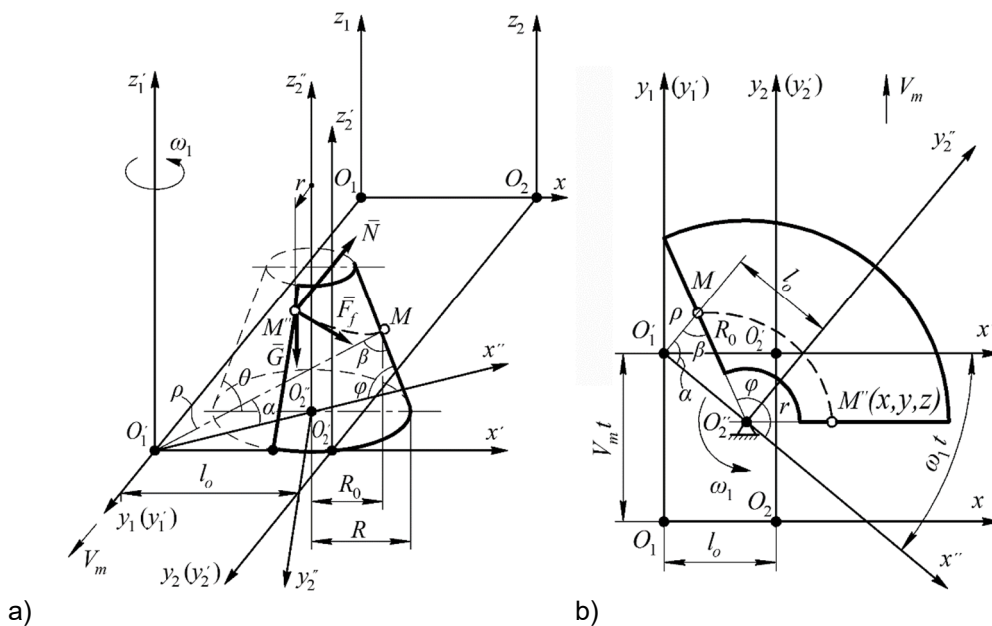


**Figure 2.** Equivalent schematic model of motion performed by material point  $M$  on cone-shaped surface of rotor's lower vane: a) position of vane in three-dimensional Cartesian coordinate system  $O_1x_1y_1z_1$ ; b) position of vane in two-dimensional Cartesian coordinate system  $O_1x_1y_1$ .

The following elements of the model are shown in the diagrams presented in Fig. 2:  $M$  – random material point (soil particle) moving along the vane;  $R_0$  – initial radius of the point  $M$ ;  $r$  – radius of the point  $M$  at the moment of its departure from the vane;  $\rho$  – polar radius of the point  $M$ ;  $\varphi$  – angular coordinate defining the position of the material point  $M$  on the surface of the vane at an arbitrary instant of time  $t$ ;  $\alpha$  – angle between the polar radius and the axis  $x''$ ;  $\beta$  – angle between the polar radius and the initial radius of the material point  $M$ .

The absolute coordinate system  $O_1x_1y_1z_1$  and the moving coordinate system  $O_2x_2y_2z_2$  with the rotation axis  $O_1z_1$  are selected in such a way that the moving coordinate system is rigidly bound with the vane and moves together with it relative to the absolute coordinate system in translation along the axis  $O_1y_1$ , rotating at the same time about the axis  $O_1z_1$ . Further, the system of coordinates  $O_2''x_2''y_2''z_2''$  is introduced for the rotation of the conical surface itself about the axis  $O_2''z_2''$  up to the moment, when the soil clod departs from the surface of the cone.

In view of the fact that the working surface of the vane is at an angle of  $\Theta$  to the horizon and is limited by the borders of the lower and upper bases of the cone, the soil particle can be placed on this surface at an arbitrary position and its motion path can be considered as the path of the motion performed by the material point  $M$  along the vane with the support of the horizontal plane (Vasilenko, 1996).

It is assumed that the coordinates of the moving material point  $M$  relative to the absolute coordinate system  $O_1x_1y_1z_1$  are equal to  $x$ ,  $y$  and  $z$ , i.e.  $M(x, y, z)$ .

In order to investigate the kinematics of the motion performed by the material point  $M$  along the working surface of the vane, it is necessary to generate the equation of the cone-shaped vane surface with reference to the absolute coordinate system  $O_1x_1y_1z_1$ . It is effectively a constraint equation of the following form:

$$f(x, y, z, t) = [x + l_0 \cdot \cos(\omega_1 t)]^2 + [y - V_m t + l_0 \cdot \sin(\omega_1 t)]^2 - (R \cdot \tan \Theta - z)^2 = 0, \quad (1)$$

where  $t$  – current time [s];  $l_0$  – distance between the axes  $y_1$  and  $y_2$ , [m];  $\omega_1$  – angular velocity of the lower beater [ $s^{-1}$ ];  $R$  – radius of the lower base of the cone [m];  $\Theta$  – angle between the cone's generator and its lower base [deg].

Further, the system of the parametric equations that describe the motion of the material point  $M$  on the working surface of the vane with reference to the absolute coordinate system  $O_1x_1y_1z_1$  has to be generated:

$$\left. \begin{aligned} x &= r \cdot \cos(\varphi + \omega_1 t) - l_0 \cdot \cos(\omega_1 t), \\ y &= V_m t + r \cdot \sin(\varphi + \omega_1 t) - l_0 \cdot \sin(\omega_1 t), \\ z &= \tan \Theta \cdot (R_0 - r). \end{aligned} \right\} \quad (2)$$

where  $r$  – radius of the circle at the height corresponding to the  $z$  coordinate of the material point  $M$  [m];  $\varphi$  – angular coordinate that defines the position of the material point  $M$  on the working surface of the vane at an arbitrary instant of time  $t$  during the rotation [deg].

For the purpose of generating the differential equation of the motion performed by the soil particle relative to the absolute coordinate system  $O_1x_1y_1z_1$  on the cone-shaped surface of the vane, Lagrange's dynamic equations of the first kind can be used (Vasilenko, 1996).

$$\left. \begin{aligned} m\ddot{x} &= \sum_{k=1}^n F_{kx} + \frac{\partial f}{\partial x} \lambda, \\ m\ddot{y} &= \sum_{k=1}^n F_{ky} + \frac{\partial f}{\partial y} \lambda, \\ m\ddot{z} &= \sum_{k=1}^n F_{kz} + \frac{\partial f}{\partial z} \lambda. \end{aligned} \right\} \quad (3)$$

where  $m$  – mass of the soil particle [kg];  $\ddot{x}$ ,  $\ddot{y}$  and  $\ddot{z}$  – projections of the soil particle acceleration on the respective coordinate axes [ $m \cdot s^{-2}$ ];  $\lambda$  – Lagrange's undetermined multiplier;  $\sum_{k=1}^n F_{kx}$ ,  $\sum_{k=1}^n F_{ky}$  and  $\sum_{k=1}^n F_{kz}$  – algebraic sum of the projections of the force acting on the soil particle [N].

Taking into account the equivalent schematic model (Fig. 2), the following system of differential equations is obtained:

$$\left. \begin{aligned} m\ddot{x} &= F_{fx} + \frac{\partial f}{\partial x} \lambda, \\ m\ddot{y} &= F_{fy} + \frac{\partial f}{\partial y} \lambda, \\ m\ddot{z} &= F_{fz} - mg + \frac{\partial f}{\partial z} \lambda. \end{aligned} \right\} \quad (4)$$

where  $F_{fx}$ ,  $F_{fy}$  and  $F_{fz}$  – projections of the friction forces  $\bar{F}_f$  on the coordinate axes  $O_1x$ ,  $O_1y_1$ ,  $O_1z_1$ , respectively;  $g$  – acceleration of gravity [ $m \cdot s^{-2}$ ].

The next step is to find the partial derivatives that are present in the system of Eqs (4). For that purpose, the parametric equation of the surface (1), i.e. the constraint equation, has to be differentiated with respect to the respective coordinates. The following is obtained:

$$\left. \begin{aligned} \frac{\partial f}{\partial x} &= 2[x + l_0 \cdot \cos(\omega_1 t)], \\ \frac{\partial f}{\partial y} &= 2[y - V_m t + l_0 \cdot \sin(\omega_1 t)], \\ \frac{\partial f}{\partial z} &= 2(R \cdot \tan \Theta - z). \end{aligned} \right\} \quad (5)$$

After substituting for  $x$ ,  $y$  and  $z$  in the obtained partial derivatives (5) their parametric Eqs (2), the following expressions for the partial derivatives are arrived at:

$$\left. \begin{aligned} \frac{\partial f}{\partial x} &= 2[r \cdot \cos(\varphi + \omega_1 t) - l_0 \cdot \cos(\omega_1 t) + l_0 \cdot \cos(\omega_1 t)] = 2r \cdot \cos(\varphi + \omega_1 t), \\ \frac{\partial f}{\partial y} &= 2[V_m t + r \cdot \sin(\varphi + \omega_1 t) - l_0 \cdot \sin(\omega_1 t) - V_m t + l_0 \cdot \sin(\omega_1 t)] = \\ &= 2r \cdot \sin(\varphi + \omega_1 t), \\ \frac{\partial f}{\partial z} &= 2(R - R_0 + r) \cdot \tan \Theta. \end{aligned} \right\} \quad (6)$$

By substituting the expressions (6) into the system of differential Eqs (3), the following is obtained:

$$\left. \begin{aligned} m\ddot{x} &= F_{f_x} + 2r \cdot \cos(\varphi + \omega_1 t) \cdot \lambda, \\ m\ddot{y} &= F_{f_y} + 2r \cdot \sin(\varphi + \omega_1 t) \cdot \lambda, \\ m\ddot{z} &= F_{f_z} - mg + 2(R - R_0 + r) \cdot \tan\Theta \cdot \lambda. \end{aligned} \right\} \quad (7)$$

At the same time, the force of friction  $\bar{F}_f$  is determined, as is known, in accordance with the Coulomb's law with the use of the following expression:

$$F_f = f \cdot N \quad (8)$$

where  $N$  – normal reaction of the constraint (in this case, the vane surface);  $f$  – coefficient of friction.

The friction force projections  $\bar{F}_{f_x}$ ,  $\bar{F}_{f_y}$ ,  $\bar{F}_{f_z}$  on the coordinate axes are determined in accordance with the following well-known expressions:

$$F_{f_x} = F_f \cdot \frac{\dot{x}}{\sqrt{\dot{x}^2 + \dot{y}^2 + \dot{z}^2}}, \quad (9)$$

$$F_{f_y} = F_f \cdot \frac{\dot{y}}{\sqrt{\dot{x}^2 + \dot{y}^2 + \dot{z}^2}}, \quad (10)$$

$$F_{f_z} = F_f \cdot \frac{\dot{z}}{\sqrt{\dot{x}^2 + \dot{y}^2 + \dot{z}^2}}. \quad (11)$$

Moreover, in accordance with Vasilenko (1998) the following expression holds true:

$$N = \Delta \cdot \lambda, \quad (12)$$

where  $\Delta$  – modulus of the gradient of the function defined by the constraint equation.

According to Vasilenko (1998):

$$\Delta = \sqrt{\left(\frac{\partial f}{\partial x}\right)^2 + \left(\frac{\partial f}{\partial y}\right)^2 + \left(\frac{\partial f}{\partial z}\right)^2} \quad (13)$$

On the basis of the above considerations, it becomes possible to write the expressions (9) – (11) in the following form:

$$F_{f_x} = f \cdot \Delta \cdot \lambda \cdot \frac{\dot{x}}{\sqrt{\dot{x}^2 + \dot{y}^2 + \dot{z}^2}}, \quad (14)$$

$$F_{f_y} = f \cdot \Delta \cdot \lambda \cdot \frac{\dot{y}}{\sqrt{\dot{x}^2 + \dot{y}^2 + \dot{z}^2}}, \quad (15)$$

$$F_{f_z} = f \cdot \Delta \cdot \lambda \cdot \frac{\dot{z}}{\sqrt{\dot{x}^2 + \dot{y}^2 + \dot{z}^2}}. \quad (16)$$

By substituting the obtained expressions (14) – (16) into the system of Eqs (7), the following system of differential equations is obtained:

$$\left. \begin{aligned} m\ddot{x} &= \lambda \cdot \left[ 2r \cdot \cos(\varphi + \omega_1 t) + f \cdot \Delta \cdot \frac{\dot{x}}{\sqrt{\dot{x}^2 + \dot{y}^2 + \dot{z}^2}} \right], \\ m\ddot{y} &= \lambda \cdot \left[ 2r \cdot \sin(\varphi + \omega_1 t) + f \cdot \Delta \cdot \frac{\dot{y}}{\sqrt{\dot{x}^2 + \dot{y}^2 + \dot{z}^2}} \right], \\ m\ddot{z} &= \lambda \cdot \left[ 2(R - R_0 + r) \cdot \tan \Theta + f \cdot \Delta \cdot \frac{\dot{z}}{\sqrt{\dot{x}^2 + \dot{y}^2 + \dot{z}^2}} \right] - mg. \end{aligned} \right\} \quad (17)$$

After that, Lagrange's multiplier is derived from the first equation in the system (17). Its value is as follows:

$$\lambda = \frac{m\ddot{x}}{2r \cdot \cos(\varphi + \omega_1 t) + f \cdot \Delta \cdot \frac{\dot{x}}{\sqrt{\dot{x}^2 + \dot{y}^2 + \dot{z}^2}}} \quad (18)$$

The obtained value of the multiplier  $\lambda$ , as per expression (18), is substituted into the second and third equations of the system (17), which results in the following:

$$\left. \begin{aligned} m\ddot{y} &= \frac{m\ddot{x}}{2r \cdot \cos(\varphi + \omega_1 t) + f \cdot \Delta \cdot \frac{\dot{x}}{\sqrt{\dot{x}^2 + \dot{y}^2 + \dot{z}^2}}} \times \\ &\times \left[ 2r \cdot \sin(\varphi + \omega_1 t) + f \cdot \Delta \cdot \frac{\dot{y}}{\sqrt{\dot{x}^2 + \dot{y}^2 + \dot{z}^2}} \right], \\ m\ddot{z} &= \frac{m\ddot{x}}{2r \cdot \cos(\varphi + \omega_1 t) + f \cdot \Delta \cdot \frac{\dot{x}}{\sqrt{\dot{x}^2 + \dot{y}^2 + \dot{z}^2}}} \times \\ &\times \left[ 2(R - R_0 + r) \cdot \tan \Theta + f \cdot \Delta \cdot \frac{\dot{z}}{\sqrt{\dot{x}^2 + \dot{y}^2 + \dot{z}^2}} \right] - mg. \end{aligned} \right\} \quad (19)$$

The system of differential Eqs (19) is just the desired system of differential equations describing the motion of the soil particle on the conical surface of the lower beater.

However, in order to solve the above system of differential equations, it is necessary to transform it into the parametric form. For that purpose, each component of the system of equations (19) has to be transformed into the parametric form.

As the system of equations (19) contains the second derivatives of the coordinates with time, that is:  $\ddot{x}$ ,  $\ddot{y}$ ,  $\ddot{z}$ , these derivatives have to be derived from the system of equations (2) by means of their twofold differentiation.

After the first differentiation of the above-mentioned equations, the following expressions are obtained for the first-order derivatives:

$$\left. \begin{aligned} \dot{x} &= \dot{r} \cdot \cos(\varphi + \omega_1 t) - r \cdot (\dot{\varphi} + \omega_1) \cdot \sin(\varphi + \omega_1 t) + l_0 \cdot \omega_1 \cdot \sin(\omega_1 t), \\ \dot{y} &= V_m + \dot{r} \cdot \sin(\varphi + \omega_1 t) + r \cdot (\dot{\varphi} + \omega_1) \cdot \cos(\varphi + \omega_1 t) + l_0 \cdot \omega_1 \cdot \cos(\omega_1 t), \\ \dot{z} &= \tan \Theta \cdot (-\dot{r}) = -\dot{r} \cdot \tan \Theta, \end{aligned} \right\} \quad (20)$$

where  $\dot{r}$  – projection of the velocity of the position vector  $\vec{r}$  on its direction;  $\dot{\varphi}$  – projection of the angular velocity on the perpendicular to the position vector  $\vec{r}$ .

After the second differentiation of the equations under consideration, the following expressions are obtained for the second derivatives:

$$\left. \begin{aligned} \ddot{x} &= \ddot{r} \cdot \cos(\varphi + \omega_1 t) - \dot{r} \cdot (\dot{\varphi} + \omega_1) \cdot \sin(\varphi + \omega_1 t) - \dot{r} \cdot (\dot{\varphi} + \omega_1) \cdot \sin(\varphi + \omega_1 t) - \\ &\quad - r \cdot \ddot{\varphi} \cdot \sin(\varphi + \omega_1 t) - r \cdot (\dot{\varphi} + \omega_1)^2 \cdot \cos(\varphi + \omega_1 t) + l_0 \cdot \omega_1^2 \cdot \cos(\omega_1 t), \\ \ddot{y} &= \ddot{r} \cdot \sin(\varphi + \omega_1 t) + \dot{r} \cdot (\dot{\varphi} + \omega_1) \cdot \cos(\varphi + \omega_1 t) + \dot{r} \cdot (\dot{\varphi} + \omega_1) \cdot \cos(\varphi + \omega_1 t) + \\ &\quad + r \cdot \ddot{\varphi} \cdot \cos(\varphi + \omega_1 t) - r \cdot (\dot{\varphi} + \omega_1)^2 \cdot \sin(\varphi + \omega_1 t) + l_0 \cdot \omega_1^2 \cdot \sin(\omega_1 t), \\ \ddot{z} &= -\ddot{r} \cdot \tan \Theta. \end{aligned} \right\} \quad (21)$$

Further, in accordance with (13), the gradient of the function defined by the constraint equation is determined by substituting the expressions (5) into (13). The result is:

$$\Delta = 2\sqrt{[x + l_0 \cdot \cos(\omega_1 t)]^2 + [y - V_m t + l_0 \cdot \sin(\omega_1 t)]^2 + (R \cdot \tan \Theta - z)^2}. \quad (22)$$

After substituting for  $x$ ,  $y$  and  $z$  in the expression (22) their expressions (2) and carrying out a number of transformations, the following is obtained:

$$\Delta = 2\sqrt{r^2 + (R - R_0 + r)^2 \cdot \tan^2 \Theta}. \quad (23)$$

Also, the expressions contained in (9), (10) and (11) have to be determined with the use of the expressions (20). First, the following designation is introduced:

$$\sqrt{\dot{x}^2 + \dot{y}^2 + \dot{z}^2} = A. \quad (24)$$

Then, taking into account (20), the following is obtained:

$$\begin{aligned} A &= \sqrt{[\dot{r} \cdot \cos(\varphi + \omega_1 t) - r \cdot (\dot{\varphi} + \omega_1) \cdot \sin(\varphi + \omega_1 t) + l_0 \cdot \omega_1 \cdot \sin(\omega_1 t)]^2 + \\ &\quad + [V_m + \dot{r} \cdot \sin(\varphi + \omega_1 t) + r \cdot (\dot{\varphi} + \omega_1) \cdot \cos(\varphi + \omega_1 t) + l_0 \cdot \omega_1 \cdot \cos(\omega_1 t)]^2 + \\ &\quad + (-\dot{r} \cdot \tan \Theta)^2}. \end{aligned} \quad (25)$$

Consequently:

$$\begin{aligned} \frac{\dot{x}}{\sqrt{\dot{x}^2 + \dot{y}^2 + \dot{z}^2}} &= \frac{\dot{x}}{A} = \\ &= \frac{\dot{r} \cdot \cos(\varphi + \omega_1 t) - r \cdot (\dot{\varphi} + \omega_1) \cdot \sin(\varphi + \omega_1 t) + l_0 \cdot \omega_1 \cdot \sin(\omega_1 t)}{A}, \end{aligned} \quad (26)$$

$$\begin{aligned} \frac{\dot{y}}{\sqrt{\dot{x}^2 + \dot{y}^2 + \dot{z}^2}} &= \frac{\dot{y}}{A} = \\ &= \frac{V_m + \dot{r} \cdot \sin(\varphi + \omega_1 t) + r \cdot (\dot{\varphi} + \omega_1) \cdot \cos(\varphi + \omega_1 t) + l_0 \cdot \omega_1 \cdot \cos(\omega_1 t)}{A}, \end{aligned} \quad (27)$$

$$\frac{\dot{z}}{\sqrt{\dot{x}^2 + \dot{y}^2 + \dot{z}^2}} = \frac{\dot{z}}{A} = -\frac{\dot{r} \cdot \tan \Theta}{A} \quad (28)$$

By substituting the expressions (21), (23), (26)–(28) into the respective expressions in the system of equations (19), the system of differential equations in the unknown  $r$  and  $\varphi$  is arrived at, which has to be solved by numerical methods on the PC.

In case of the upper beater vane, the motions to be given consideration are the clockwise rotary motion at a constant angular velocity of  $\omega_2$  in the horizontal plane as well as the uniform translation motion together with the potato harvester with reference

to the absolute coordinate system  $O_1xy_1$ . The diagram of the position of the soil particle  $M$  on the working surface of the cylindrical vane offset with respect to the vertical rotation axis  $O_1z_1$  (point  $O_1$ ) and the forces acting on it are presented in Fig. 3.

In the schematic model presented in Fig. 3, the following forces are shown:  $N$  – normal reaction of the constraint;  $F_f$  – force of friction. The designations are as follows:  $V$  – radial velocity of the particle;  $O_1xy_1$  – absolute (fixed) coordinate system;  $O_2xy_2$  – moving coordinate system that is rigidly bound with the vane and moves together with it with reference to the absolute coordinate system  $O_1xy_1$  in translation along the  $O_1y_1$  axis and simultaneously in rotation about the  $O_1z_1$  axis (point  $O_1$ ). The coordinate system  $O'_1x'y'_1$  moves together with the vane along the  $O_1y_1$  axis at the potato harvester's translation velocity  $V_m$  in such a way that its axis  $O'_1x'$  remains always parallel to the  $O_1x$  axis and it plays an ancillary part (for convenience in the representation of angles in Fig. 3 at an arbitrary instant of time  $t$ ); the coordinate system  $O''_2x''y''_2$  is introduced for the purpose of analysing the rotation of the cylindrical vane itself about the  $O''_2z''_2$  axis (point  $O''_2$ ).

The displacement of the soil particle on the working surface of the cylindrical vane is assumed to be the motion of the material point  $M$  relative to the fixed coordinate system  $O_1xy_1$ . In order to analyse the kinematics of the motion performed by the material point  $M$  on the working surface of the cylindrical vane, it is necessary to generate the respective vane surface equation, i.e. the constraint equation, which appears as follows:

$$f(x, y, t) = [x + l_0 \cos(\omega_2 t)]^2 + [y - V_m t + l_0 \sin(\omega_2 t)]^2 - R_0^2 = 0, \quad (29)$$

where  $\omega_2$  – angular velocity of the upper beater [ $s^{-1}$ ].

The parametric equations describing the motion of the material point  $M$  on the working surface of the vane relative to the fixed coordinate system  $O_1xy_1$  have the following form:

$$\left. \begin{aligned} x &= R_0 \cdot \left[ \cos(\varphi + \omega_2 t) - \frac{l_0}{R_0} \cdot \cos(\omega_2 t) \right], \\ y &= V_m t + R_0 \cdot \left[ \sin(\varphi + \omega_2 t) - \frac{l_0}{R_0} \cdot \sin(\omega_2 t) \right], \end{aligned} \right\} \quad (30)$$

where  $\varphi$  – angular coordinate of the material point  $M$ ;  $x, y$  – absolute coordinates of the material point  $M$  moving on the surface of the vane.

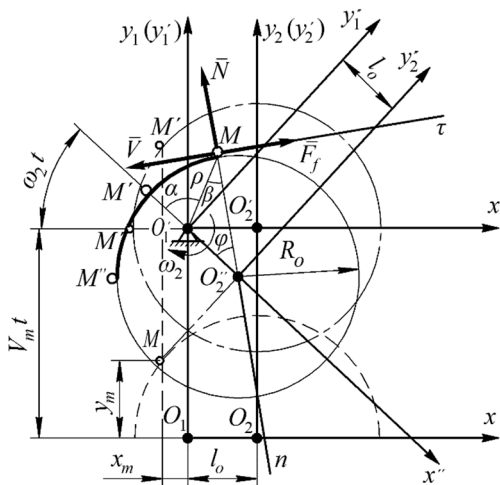


**Figure 3.** Schematic model of interaction between soil particle  $M$  and working surface of cylindrical vane in upper beater.

The derivative  $\dot{\varphi}$ , the same as the function  $\varphi$  itself, are to be determined with the use of the respective dynamic equations. For that purpose, the Lagrange's equations of the second kind can be used. The angular coordinate  $\varphi$  is taken as the generalised coordinate.

The Lagrange's equation of the second kind in the generalised coordinate  $\varphi$  appears as follows:

$$\frac{d}{dt} \frac{\partial T}{\partial \dot{\varphi}} - \frac{\partial T}{\partial \varphi} = Q_{\varphi} \quad (31)$$

where  $T$  – kinetic energy of the material point;  $\varphi$  – generalised coordinate;  $\dot{\varphi}$  – generalised velocity;  $Q_{\varphi}$  – generalised force corresponding to the generalised coordinate  $\varphi$ .

With the use of the expression (30), the kinetic energy  $T$  of the material point  $M$  can be expressed in terms of the generalised velocity. The result is as follows:

$$T = \frac{m \cdot (\dot{x}^2 + \dot{y}^2)}{2}. \quad (32)$$

The following expressions are obtained for the derivatives  $\dot{x}$ ,  $\dot{y}$ :

$$\left. \begin{aligned} \dot{x} &= R_0 \left[ -(\dot{\varphi} + \omega_2) \cdot \sin(\varphi + \omega_2 t) + \frac{l_0}{R_0} \cdot \omega_2 \cdot \sin(\omega_2 t) \right], \\ \dot{y} &= V_m + R_0 \left[ (\dot{\varphi} + \omega_2) \cdot \cos(\varphi + \omega_2 t) - \frac{l_0}{R_0} \cdot \omega_2 \cdot \cos(\omega_2 t) \right]. \end{aligned} \right\} \quad (33)$$

Taking into account the equation (31) and the expressions (32) and (33), the partial derivatives of the  $\dot{x}^2$  and  $\dot{y}^2$  expressions with respect to the generalised coordinate  $\varphi$  are obtained:

$$\left. \begin{aligned} \frac{\partial \dot{x}^2}{\partial \varphi} &= R_0^2 \left[ 2(\dot{\varphi} + \omega_2)^2 \cdot \sin(\varphi + \omega_2 t) \cdot \cos(\varphi + \omega_2 t) - \right. \\ &\quad \left. - 2 \cdot \frac{l_0}{R_0} \cdot \omega_2 \cdot (\dot{\varphi} + \omega_2) \cdot \sin(\omega_2 t) \cdot \cos(\varphi + \omega_2 t) \right], \\ \frac{\partial \dot{y}^2}{\partial \varphi} &= -2R_0^2 \cdot (\dot{\varphi} + \omega_2)^2 \cdot \cos(\varphi + \omega_2 t) \cdot \sin(\varphi + \omega_2 t) + \\ &\quad + 2R_0^2 \cdot \frac{l_0}{R_0} \cdot \omega_2 \cdot (\dot{\varphi} + \omega_2) \cdot \cos(\omega_2 t) \cdot \sin(\varphi + \omega_2 t) - \\ &\quad - 2V_m \cdot R_0 \cdot (\dot{\varphi} + \omega_2) \cdot \sin(\varphi + \omega_2 t). \end{aligned} \right\} \quad (34)$$

The partial derivatives of  $\dot{x}^2$  and  $\dot{y}^2$  with respect to the generalised velocity  $\dot{\varphi}$  appear as follows:

$$\left. \begin{aligned} \frac{\partial \dot{x}^2}{\partial \dot{\varphi}} &= R_0^2 \left[ 2(\dot{\varphi} + \omega_2) \cdot \sin^2(\varphi + \omega_2 t) - 2 \frac{l_0}{R_0} \cdot \omega_2 \cdot \sin(\omega_2 t) \cdot \sin(\varphi + \omega_2 t), \right] \\ \frac{\partial \dot{y}^2}{\partial \dot{\varphi}} &= 2R_0^2 \cdot (\dot{\varphi} + \omega_2) \cdot \cos^2(\varphi + \omega_2 t) - 2R_0^2 \cdot \frac{l_0}{R_0} \cdot \omega_2 \cdot \cos(\omega_2 t) \cdot \cos(\varphi + \omega_2 t) + \\ &\quad + 2V_m \cdot R_0 \cdot \cos(\varphi + \omega_2 t). \end{aligned} \right\} \quad (35)$$

Taking into account the Eq. (31) as well as the expressions (34) and (35), after a number of transformations the following expressions can be obtained:

$$\left. \begin{aligned} \frac{d}{dt} \left( \frac{\partial \dot{x}^2}{\partial \dot{\varphi}} \right) - \frac{\partial \dot{x}^2}{\partial \varphi} &= 2R_0^2 \cdot \ddot{\varphi} \cdot \sin^2(\varphi + \omega_2 t) + R_0^2 \cdot (\varphi + \omega_2)^2 \cdot \sin^2(\varphi + \omega_2 t) - \\ &- 2 \frac{l_0}{R_0} \cdot \omega_2^2 \cdot R_0^2 \cdot \cos(\omega_2 t) \cdot \sin(\varphi + \omega_2 t), \\ \frac{d}{dt} \left( \frac{\partial \dot{y}^2}{\partial \dot{\varphi}} \right) - \frac{\partial \dot{y}^2}{\partial \varphi} &= 2R_0^2 \cdot \ddot{\varphi} \cdot \cos^2(\varphi + \omega_2 t) - R_0^2 \cdot (\varphi + \omega_2)^2 \cdot \sin^2(\varphi + \omega_2 t) + \\ &+ 2 \frac{l_0}{R_0} \cdot \omega_2^2 \cdot R_0^2 \cdot \sin(\omega_2 t) \cdot \cos(\varphi + \omega_2 t). \end{aligned} \right\} \quad (36)$$

Finally, the left side of the Eq. (31) obtains the following form after substituting into it the expressions (36):

$$\begin{aligned} \frac{d}{dt} \left( \frac{\partial T}{\partial \dot{\varphi}} \right) - \frac{\partial T}{\partial \varphi} &= \frac{m}{2} \cdot \frac{d}{dt} \left( \frac{\partial \dot{x}^2}{\partial \dot{\varphi}} \right) + \frac{d}{dt} \left( \frac{\partial \dot{y}^2}{\partial \dot{\varphi}} \right) - \left( \frac{\partial \dot{x}^2}{\partial \varphi} + \frac{\partial \dot{y}^2}{\partial \varphi} \right) = \\ &= \frac{m}{2} \left\{ 2R_0^2 \cdot [\sin^2(\varphi + \omega_2 t) + \cos^2(\varphi + \omega_2 t)] \ddot{\varphi} + \right. \\ &+ 2R_0^2 \cdot \frac{l_0}{R_0} \cdot \omega_2^2 \cdot [\sin(\omega_2 t) \cdot \cos(\varphi + \omega_2 t) - \cos(\omega_2 t) \cdot \sin(\varphi + \omega_2 t)] \left. \right\} = \\ &= \frac{m}{2} \left\{ 2R_0^2 \cdot \ddot{\varphi} + 2R_0^2 \cdot \frac{l_0}{R_0} \cdot \omega_2^2 \cdot \left[ \sin(\omega_2 t) \cdot \left( \cos \varphi \cdot \cos(\omega_2 t) - \right. \right. \right. \\ &\left. \left. \left. - \sin \varphi \cdot \sin(\omega_2 t) \right) - \cos(\omega_2 t) \cdot \left( \sin \varphi \cdot \cos(\omega_2 t) + \cos \varphi \cdot \sin(\omega_2 t) \right) \right] \right\} = \\ &= \frac{m}{2} \left[ 2R_0^2 \cdot \ddot{\varphi} + 2R_0^2 \cdot \frac{l_0}{R_0} \cdot \omega_2^2 \cdot \left( -\sin^2(\omega_2 t) \cdot \sin \varphi - \cos^2(\omega_2 t) \cdot \sin \varphi \right) \right] = \\ &= \frac{m}{2} \left[ 2R_0^2 \cdot \ddot{\varphi} - 2R_0^2 \cdot \frac{l_0}{R_0} \cdot \omega_2^2 \cdot \sin \varphi \right]. \end{aligned} \quad (37)$$

In this case, the generalised force is the moment of friction  $M_{z_1}(\bar{F}_f)$  with respect to the axis  $O_1z_1$ , which is determined in accordance with the following expression:

$$M_{z_1}(\bar{F}_f) = F_f \cdot N \cdot R_0, \quad (38)$$

where  $N$  – normal reaction of the constraint surface;  $f$  – coefficient of friction;  $R_0$  – radius of the cylindrical vane.

In order to determine the force of friction, it is necessary to determine the normal reaction  $N$  of the cylindrical vane, which in the general case can be represented by the following expression:

$$N = m \cdot \frac{Df(x, y, t)}{|\text{grad } f|}, \quad (39)$$

where  $m$  – mass of the soil particle [kg];  $D$  – differential operator (Vasilenko, 1998).

In the expression (39), the numerator and the denominator have to be determined. The following expressions have been obtained for them:

$$\begin{aligned}
Df(x, y, t) &= 2 \left\{ \left[ \dot{x} - \omega_2 \cdot l_0 \cdot \sin(\omega_2 t) \right]^2 + \right. \\
&+ \left[ \dot{y} - V_m + \omega_2 \cdot l_0 \cdot \cos(\omega_2 t) \right]^2 + \\
&+ \left[ x + l_0 \cdot \cos(\omega_2 t) \right] \cdot \left[ -l_0 \cdot \omega_2^2 \cdot \cos(\omega_2 t) \right] - \\
&- l_0 \cdot \omega_2^2 \cdot \sin(\omega_2 t) \cdot \left[ y - V_m t + l_0 \cdot \sin(\omega_2 t) \right] \left. \right\} = \\
&= 2R_0 \left[ R_0 \cdot (\dot{\varphi} + \omega_2)^2 - l_0 \cdot \omega_2^2 \cdot \cos \varphi \right],
\end{aligned} \tag{40}$$

and:

$$\begin{aligned}
|\text{grad } f| &= \sqrt{\left( \frac{df}{dx} \right)^2 + \left( \frac{df}{dy} \right)^2} = \\
&= \sqrt{4 \left[ x + l_0 \cdot \cos(\omega_2 t) \right]^2 + 4 \left[ y - V_m t + l_0 \cdot \sin(\omega_2 t) \right]^2} = 2R_0.
\end{aligned} \tag{41}$$

After substituting the expressions (40) and (41) into the expression (39), the following expression is obtained for the normal reaction  $N$ :

$$N = m \left[ l_0 \cdot \omega_2^2 \cdot \cos \varphi - R_0 \cdot (\dot{\varphi} + \omega_2)^2 \right]. \tag{42}$$

Taking into account the expressions (31), (37) and (42), the following differential equation is obtained for describing the motion of a soil particle on the cylindrical surface of the upper beater vane offset with respect to the vertical rotation axis with due account for the friction forces:

$$R_0^2 \left( \ddot{\varphi} - \frac{l_0}{R_0} \cdot \omega_2^2 \cdot \sin \varphi \right) = f_f \left[ R_0 (\dot{\varphi} + \omega_2)^2 - l_0 \cdot \omega_2^2 \cdot \cos \varphi \right] R_0 \tag{43}$$

or

$$\ddot{\varphi} = \frac{l_0}{R_0} \cdot \omega_2^2 \cdot \sin \varphi + f_f \left[ (\dot{\varphi} + \omega_2)^2 - \frac{l_0}{R_0} \cdot \omega_2^2 \cdot \cos \varphi \right]. \tag{44}$$

The initial conditions for solving the differential Eq. (44) are as follows:  
at  $t = 0$ :

$$\begin{aligned}
\varphi_0 &= 0, \\
\dot{\varphi}_0 &= \frac{V_m}{R_0} - \omega_2 \left( 1 - \frac{l_0}{R_0} \right).
\end{aligned} \tag{45}$$

The condition of the soil particle motion in constant contact with the working surface of the cylinder-shaped vane is represented by the following in equation:

$$\frac{N}{m \cdot R_0} = \omega_2^2 \cdot \frac{l_0}{R_0} \cdot \cos \varphi - (\dot{\varphi} + \omega_2)^2 \geq 0. \tag{46}$$

After substituting the numerical data into the above relations, it is possible to obtain their solutions and analyse the effect that the design and kinematic parameters of the rotor vanes have on the process of breaking the tuber-bearing soil bed.

## RESULTS

Further, the calculations carried out in the Mathcad environment with regard to the cylindrical vane are described.

The kinematic parameters of the motion performed by the soil particle on the working surface of the cylindrical vane have the following numerical values:

$$R_0 = 0.5 \text{ m};$$

$$l_0 = 0.3 \text{ m}; n = 50 \text{ min}^{-1};$$

$$V_m = 1.38 \text{ m s}^{-1}; \omega_2 = 5.23 \text{ s}^{-1}.$$

The initial conditions defined by the Eqs (30) and (33) at the moment of time  $t = 0$  appear as follows:

$$x(0) = R - l_0,$$

$$x'(0) = 0,$$

$$y(0) = 0,$$

$$y'(0) = 0,$$

With the use of the parametric Eqs (30), the trajectory of the motion performed by the material point in the coordinate system  $O_1x_1y_1$  has been plotted, as is shown in Fig. 4.

It is necessary to plot graphs also for the variation of the abscissa  $x(t)$  of the material point  $M$  (Fig. 5) and its ordinate  $y(t)$  (Fig. 6) with the time  $t$ .

As is seen in the graph presented in Fig. 4, the departure of the material point  $M$  from the vane surface starts at the abscissa  $x = 0.47 \text{ m}$  and the ordinate  $y = 0.075 \text{ m}$ .

With the use of the earlier obtained expression (33), graphs can be plotted for the relations between the velocity modulus of the material point  $M$  and its velocity projections on the fixed coordinate axes  $O_1xy_1$ , on the one hand, and the time of its motion on the working surface of the vane, on the other hand (Fig. 7).

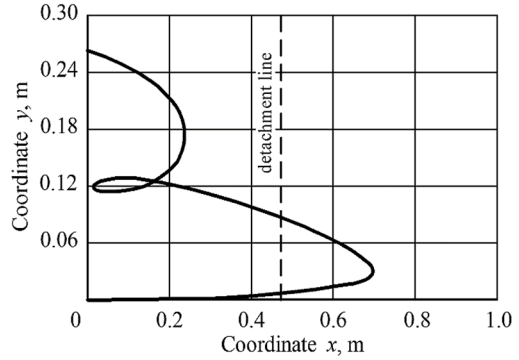


**Figure 4.** Motion path of material point  $M$  on cylindrical surface of vane in coordinate system  $O_1xy_1$ .

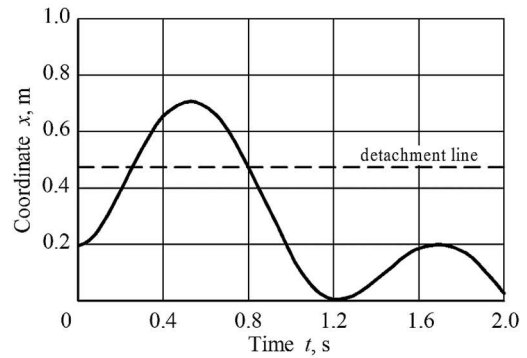


**Figure 5.** Relation between abscissa  $x$  of material point  $M$  and time  $t$ .

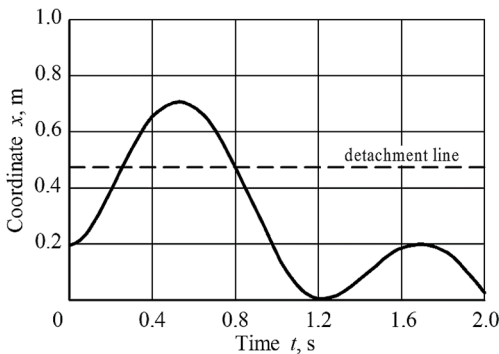


**Figure 5.** Relation between abscissa  $x$  of material point  $M$  and time  $t$ .

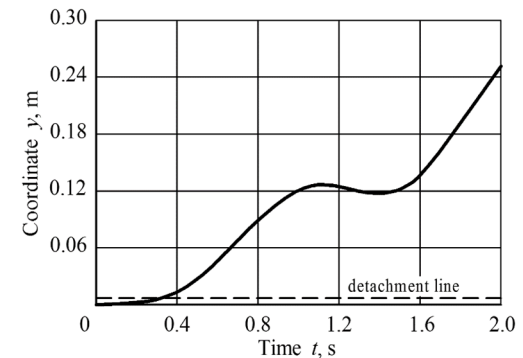


**Figure 6.** Relation between ordinate  $y$  of material point  $M$  and time  $t$ .

The modulus of the speed  $V$  of the material point in the fixed coordinate system  $O_1xy_1$  is determined with the use of the following expression:

$$V = \sqrt{(V_x)^2 + (V_y)^2} \quad (47)$$

As is obvious from the graphs presented in Fig. 7, the modulus of the speed  $V$  of the material point  $M$  shows rather unstable behaviour in terms of the interaction with the vane surface as a function of the motion time.

In order to determine the kinematic parameters of the vertical rotor's cylindrical vane, it is necessary to analyse theoretically the effect of the translation speed  $V_m$  of the motion performed by the potato harvester and the rotor rotation frequency  $n_p$  on the duration of stay of the material point on the vane surface, its absolute displacement  $s$  and the absolute speed  $V_L$  of its departure from the vane surface.

On the basis of the obtained analytical relations, after substituting the numerical values with the use of the PC, the following relation graphs have been plotted (Figs 8 and 9).

After analysing the graphs presented in Fig. 8, it becomes obvious that the absolute displacement and speed of the material point  $M$  from the zero point of the time  $t$  to the moment of its departure from the vane surface increase from 0.59 m, 1.61 m s<sup>-1</sup>, respectively, to 0.65 m, 1.81 m s<sup>-1</sup>. The greatest values of the absolute displacement and velocity of the material point  $M$  equal to 0.67 m and 1.94 m s<sup>-1</sup>, respectively, are reached at the translation speed of the potato harvester equal to 2.0 m s<sup>-1</sup>. The duration of stay of the material point  $M$  on the vane surface decreases with the increase of the translation velocity.

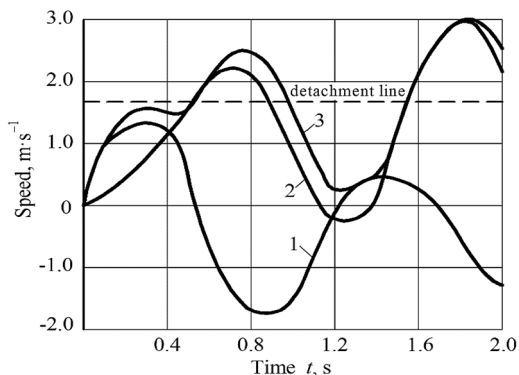


**Figure 7.** Relations between modulus of speed  $V$  of material point  $M$  (3) as well as speed projections  $V_x$  (1),  $V_y$  (2) on fixed coordinate axes  $O_1xy_1$  and time  $t$ .

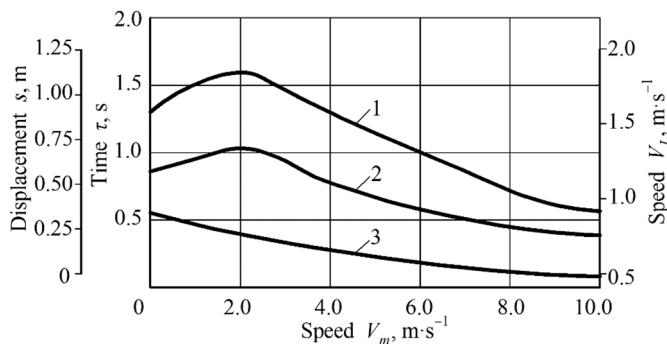


**Figure 8.** Relations between duration of stay  $\tau$  (3), absolute displacement  $s$  (2), speed  $V_L$  of departure of material point  $M$  from vane surface (1) and machine translation speed  $V_m$ .

The analysis of the relation graph presented in Fig. 9 proves that, in case of the rotor rotation frequency equal to  $20 \text{ min}^{-1}$ , the material point  $M$  does not interact with the vane surface and is in the standstill condition ( $V = 0$ ) with reference to the fixed axes  $O_1x_1y_1$ , while the initial absolute coordinates are  $x(0) = R_0 - l_0 = 0.2 \text{ m}$ ,  $y(0) = 0$ .

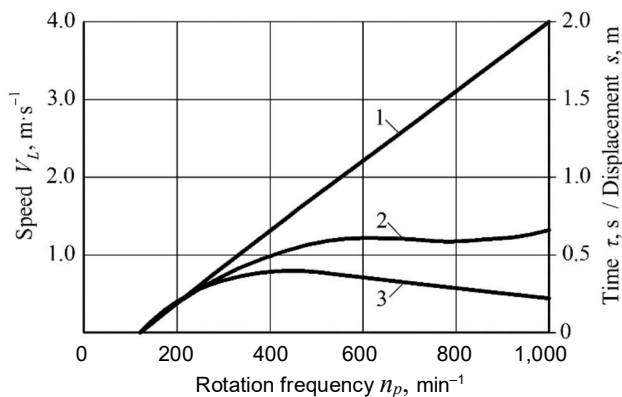


**Figure 9.** Relations between duration of stay  $\tau$  (3), absolute displacement  $s$  (2), speed  $V_L$  of departure of material point  $M$  from vane surface (1) and rotor rotation frequency  $n_p$ .

The absolute speed of the departure of the material point  $M$  from the vane surface rises to  $4 \text{ m s}^{-1}$ , when the rotor rotation frequency  $n_p$  increases in the range from  $20 \text{ min}^{-1}$  to  $100 \text{ min}^{-1}$ .

When the rotor rotation frequency  $n_p$  is within the range of  $30\text{--}40 \text{ min}^{-1}$ , the duration of the contact between the material point  $M$  and the vane reaches its maximum value equal to  $0.33 \text{ s}$ , which indicates the effective capture and transportation of parts of the potato tuber bearing soil bed by the rotor.

## CONCLUSIONS

1. The new design of a rotary tool for the potato harvester, which has a vertical axis of rotation and travels in the inter-row spacing between two adjacent potato rows, has been proposed.

2. The mathematical model of the motion of a soil particle on the working surfaces of the vanes in the rotary tool of the new design has been developed.

3. The relations have been established between the duration of stay, absolute displacement and velocity of departure from the rotor vane surface of the soil particle, on the one hand, and the rotor's kinematic and design parameters, on the other hand. For example, when the machine's translational motion velocity increases, the absolute displacement of the soil particle in the period from the zero instant of time to the moment, when the particle departs from the vane surface, rises from  $0.59 \text{ m}$  to  $0.65 \text{ m}$ , the velocity of the particle departure from the vane surface - from  $1.61 \text{ m s}^{-1}$  to  $1.81 \text{ m s}^{-1}$ . The absolute displacement and velocity of the soil particle reach their highest levels of  $0.67 \text{ m}$  and  $1.94 \text{ m s}^{-1}$ , respectively, at the translation velocity of the machine equal to  $2.0 \text{ m s}^{-1}$ . The time of the material particle staying on the vane surface decreases with the increase of the translation velocity.

4. The absolute speed of the departure of the material point from the vane surface increases to  $4 \text{ m s}^{-1}$ , as the rotor rotation frequency varies in the range from  $20 \text{ min}^{-1}$  to  $100 \text{ min}^{-1}$ .
5. The duration of the contact between the material particle and the vane reaches its maximum value equal to 0.33 s, when the rotor rotation frequency is within the range of  $30\text{--}40 \text{ min}^{-1}$ .

## REFERENCES

- Bishop, C., Rees, D., Cheema, M.U.A., Harper, G. & Stroud, G. 2012. *Potatoes*. Crop Post-Harvest: Science and Technology: Perishables. Book Chapter, pp. 179–189.
- Blahovec, J. & Židova, J. 2004. Potato bruise spot sensitivity dependence on regimes of cultivation. *Research in Agricultural Engineering* **50**(3), 89–95. doi: 10.17221/4932.RAE.
- Bulgakov, V., Bonchik, V., Holovach, I., Fedosiy, I., Volskiy, V., Melnik, V., Ihnatiev, Ye., Olt, J. 2021. Justification of parameters for novel rotary potato harvesting machine. *Agronomy Research* **19**(S2), 984–1007. doi: 10.15159/AR.21.079
- Bulgakov, V.M., Gevko, R.B., Glado, Y.B., Pavh, I.I. 1999. Theoretical justification of process of conveying and separating roots with drag conveyors. In: *Proc. National University of Agriculture*, 15–18.
- Bulgakov V., Holovach I., Ruzhylo Z., Fedosiy I., Ihnatiev Ye., Olt J. 2020. Theory of oscillations performed by tools in spiral potato separator. *Agronomy Research* **18**(1), 38–52. doi: 10.15159/AR.20.058
- Bulgakov, V., Nikolaenko, S., Adamchuk, V., Ruzhylo, Z. & Olt, J. 2018a. Theory of retaining potato bodies during operation of spiral separator. *Agronomy Research* **16**(1), 41–51. doi: 10.15159/AR.18.036
- Bulgakov, V., Nikolaenko, S., Adamchuk, V., Ruzhylo, Z. & Olt, J. 2018b. Theory of impact interaction between potato bodies and rebounding conveyor. *Agronomy Research* **16**(1), 52–64. doi: 10.15159/AR.18.037
- Bulgakov, V., Nikolaenko, S., Adamchuk, V., Ruzhylo, Z. & Olt, J. 2018c. Mathematical model of cleaning potatoes on surface of spiral separator. *Agronomy Research* **16**(4), 1590–1606. doi: 10.15159/AR.18.173
- Bulgakov, V., Pascuzzi, S., Nikolaenko, S., Santoro, F., Anifantis, A.S. & Olt, J. 2019. Theoretical study on sieving of potato heap elements in spiral separator. *Agronomy Research* **17**(1), 33–48. doi: 10.15159/AR.19.073
- Feng, B., Sun, W., Shi, L., Sun, B., Zhang, T. & Wu, J. 2017. Determination of restitution coefficient of potato tubers collision in harvest and analysis of its influence factors. *Nongye Gongcheng Xuebao/Transactions of the Chinese society of agricultural engineering* **33**(13), 50–57.
- Gao, G., Zhang, D. & Liu, J. 2011. Design of a new soil-tuber separation device on potato harvesters. *CCTA 2010: Computer and Computing Technologies in Agriculture*, IV, 604–612. doi: 10.1007/978-3-642-18354-6\_71
- Gulati, S. & Singh, M. 2019. Design and development of two row tractor operated potato combine harvester. *Potato Journal* **46**(1), 81–85.
- Hevko, R.B., Tkachenko, I.G., Synii, S.V. & Flonts, I.V. 2016. Development of design and investigation of operation process of small-scale root crop and potato harvesters. *INMATEH-Agricultural Engineering* **49**(2), 53–60.
- Ichiki, H., Nguyen Van, N. & Yoshinaga, K. 2013. Stone-clod separation and its application to potato in Hokkaido. *Engineering in Agriculture Environment and Food* **6**(2), 77–85.
- Ihnatiev, Ye., Bulgakov, V., Bonchik, V., Ruzhylo, Z., Zaryshnyak, A., Volskiy, V., Melnik, V. & Olt, J. 2021. Experimental research into operation of potato harvester with rotary tool. *Agraarteadus / Journal of Agricultural Science* **32**(1), 41–48. doi: 10.15159/jas.21.15

- Issa, I.I.M., Zhang, Z., El-Kolaly, W., Yang, X. & Wang, H. 2020. Design, ansys analysis and performance evaluation of potato digger harvester. *International Agricultural Engineering Journal* **29**(1), 60–73.
- Kheiry, A.N.O., Elssir, A., Rahma, A.E., Mohamed, M.A., Omer, E.A., Gong, H.J. & Liwei, Y. 2018. Effect of operation variables of potato digger with double chain conveyors on crop handling and machine performance. *Int. J. of Environmental & Agricultural Research* **4**(6), 87–101.
- Lü, J.Q., Sun, H., Dui, H., Peng, M.M. & Yu, J.Y. 2017. Design and experiment on conveyor separation device of potato digger under heavy soil condition. *Transactions of the CSAM* **48**(11), 146–155 (in Chinese).
- Lü, J.Q., Tian, Z.E., Yang, Y., Shang, Q.Q. & Wu, J.E. 2015. Design and experimental analysis of 4U2A type double-row potato digger. *Transactions of the CSAE* **31**(6), 17–24 (in Chinese).
- Nowak, J., Bulgakov, V., Holovach, I., Olt, J., Arak, M., Ruzhylo, Z. & Nesvidomin, A. 2019. Oscillation theory of the free ends of the spiral separator for a potato heap. In: X International Scientific Symposium FMPMSA 2019: *Farm Machinery and Process Management in Sustainable Agriculture* 157–162. doi: 10.24326/fmpmsa.2019.1.
- Olt, J., Adamchuk, V., Kornushyn, V., Melnik, V., Kaletnik, H., Ihnatiev, Ye. & Ilves, R. 2021. Research into the parameters of a potato harvester's potato heap distributor, and the justification of those parameters. *Agraarteadus / Journal of Agricultural Science* **32**(1), 92–99. doi: 10.15159/jas.21.19
- Pshechenkov, K.A., Maltsev, S.V. & Smirnov, A.V. 2018. Technology of potatoes combine harvesting on loamy soils in the Central region of Russia. *Potato and Vegetables* **4**, 19–21 (in Russian).
- Peters, R. 1997. Damage of potato tubers: A Review. *Potato Research* **39**(Spec. Issue), 479–484.
- Petrov, G. 2004. *Potato harvesting machines*. Mashinostroenije / Mechanical Engineering, Moskow, Russia, 320 pp. (in Russian).
- Ruysschaert, G., Poesen, J., Verstraeten, G. & Govers, G. 2006. Soil losses due to mechanized potato harvesting. *Soil & Tillage Research* **86**(1), 52–72. doi: 10.1016/j.still.2005.02.016.
- Ruzhylo, Z., Bulgakov, B., Adamchuk, V., Bondarchuk, A., Ihnatiev, Y., Krutyakova, V., Olt, J. 2020. Experimental research into impact of kinematic and design parameters of a spiral potato separator on quality of plant residues and soil separation. *Agraarteadus / Journal of Agricultural Science* **31**(2), 202–207. doi: 10.15159/jas.20.26.
- Siberev, A., Aksenov, A., Dorokhov, A. & Ponomarev, A. 2019. Comparative study of the force action of harvester work tools on potato tubers. *Research in Agricultural Engineering* **65**(3), 85–90. doi: 10.17221/96/2018-RAE
- Vasilenko, P.M. 1996. *Introduction to agricultural mechanics*. Kiev, Ukraine, Ed. NAU, 252 pp.
- Vasilenko, P.M. 1998. *Fundamentals of analytical methods in agricultural mechanics*. Kiev, Ukraine, Ed. NAU, 28 pp.
- Wang, X., Sun, J., Xu, Y., Li, X. & Cheng, P. 2017. Design and experiment of potato cleaning and sorting machine. *Nongye Jixie Xuebao/Transactions of the Chinese Society for Agricultural Machinery* **48**(10), 316–322 and 279.
- Wei, Z., Li, X. & Sun, C. 2017. Analysis of potato mechanical damage in harvesting and cleaning and sorting storage. *Journal of Agricultural Science and Technology* **19**(8), 63–70. doi: 10.6041/j.issn.1000-1298.2019.01.014
- Wei, Z., Li, H., Sun, C., Li, X., Su, G. & Liu, W. 2019a. Design and Experiment of Potato Combined Harvester Based on Multi-stage Separation Technology. *Nongye Jixie Xuebao/Transactions of the Chinese Society for Agricultural Machinery* **50**(1), 129–140. doi: 10.6041/j.jssn.1000-1298.2019.01.014
- Wei, Z., Li, H., Sun, C., Su, G., Liu, W. & Li, Z. 2019b. Experiments and analysis of a conveying device for soil separation and clod-crushing for a potato harvester. *Applied Engineering in Agriculture* **35**(6), 987–996. doi: 10.13031/aea.13283
- Xin, L. & Liang, J. 2017. Design of potato harvester. *Journal of Mechanical Engineering Research and Developments* **40**(2), 380–384.